Available online at www.sciencedirect.com
SCIENCE DIRECT®
PERGAMON
Applied Geochemistry 18 (2003) 1065–1080
Applied Geochemistry
www.elsevier.com/locate/apgeochem

Carbon dioxide reaction processes in a model brine aquifer at 200 °C and 200 bars: implications for geologic sequestration of carbon

John P. Kaszuba[a,*], David R. Janecky[b], Marjorie G. Snow[c]

[a]*Isotope and Nuclear Chemistry, Mail Stop J514, Los Alamos National Laboratory, Los Alamos, NM 87545, USA*
[b]*Risk Reduction and Environmental Stewardship, Mail Stop J591, Los Alamos National Laboratory, Los Alamos, NM 87545, USA*
[c]*Earth and Environmental Sciences, Mail Stop D469, Los Alamos National Laboratory, Los Alamos, NM 87545, USA*

Received 15 March 2002; accepted 11 November 2002
Editorial handling by R. Fuge

Abstract

The reactive behavior of supercritical CO_2 under conditions relevant to geologic storage and sequestration of C is largely unknown. Experiments were conducted in a flexible cell hydrothermal apparatus to determine the extent of fluid–rock reactions, in addition to carbonate mineral precipitation, that may occur in a brine aquifer–aquitard system that simulates a saline aquifer storage scenario. The system was held at 200 °C and 200 bars for 59 days (1413 h) to approach steady state, then injected with CO_2 and allowed to react for another 80 days (1924 h). In addition to magnesite precipitation, silicate minerals (quartz, plagioclase, microcline and biotite) in the aquifer and the aquitard display textures (etch pits, mineralization) indicating significant reaction. Changes in elemental abundances in the brine following addition of CO_2 include pH decrease and enrichment in Cl^-, partly due to supercritical CO_2 desiccation of the brine. Geologic sequestration systems have potential for geochemical reactions that extend beyond simple aqueous dissolution of CO_2 and precipitation of carbonate. These reactions may produce geochemical and geotechnical consequences for sequestration and provide important characteristics for monitoring and evaluation of stored CO_2. An understanding of multi-phase equilibrium relationships between supercritical CO_2 and aquifer–brine systems also raises new questions for a variety of geologic systems. Multi-phase fluid equilibria may, for example, account for the large amounts and heterogeneous distributions of calcite cement in a wide variety of geologic systems, particularly in sedimentary basin sandstones.
Published by Elsevier Science Ltd.

1. Introduction

Intense scientific and political debate surrounds the phenomenon of global warming. It is generally agreed that the burning of fossil fuels has contributed to the accumulation of CO_2 in the atmosphere, and that these increased accumulations are an important contribution to global warming (Johansson et al., 1996, and references therein). At the same time, fossil fuel energy resources are important to economic viability and national security for the foreseeable future. Carbon management is the term often used to describe the emergent policies and technologies that seek to balance energy supplied by fossil fuel with the distribution of CO_2 among atmosphere, biosphere, and geosphere.

One important potential component of C management is the capture of CO_2 emissions and subsequent emplacement of supercritical CO_2 into geologic media (Holloway, 1997a; Bachu, 2000) or the deep ocean (Harrison et al., 1995; Koide et al., 1997). Candidate

* Corresponding author.
E-mail address: jkaszuba@lanl.gov (J. P. Kaszuba).

0883-2927/03/$ - see front matter Published by Elsevier Science Ltd.
doi:10.1016/S0883-2927(02)00239-1

geologic media include saline aquifers, depleted oil/gas reservoirs, and coal formations (Bachu et al., 1994; Bergman et al., 1997; Freund and Ormerod, 1997; Holloway, 1997a,b; Hitchon et al., 1999; Holloway et al., 1999; Bachu, 2000). Retention of supercritical CO_2 presumably occurs by one or more mechanisms (Bachu et al., 1994): stratigraphic and/or structural trapping, hydrodynamic trapping, and mineral precipitation. Stratigraphic and/or structural trapping is analogous to hydrocarbon retention in petroleum reservoirs. Hydrodynamic trapping combines dissolution of supercritical CO_2 with a long residence or travel time of aqueous CO_2, on the order of thousands to a million years. Mineral precipitation involves the formation of carbonate minerals. Broadly speaking, mineral precipitation can also be referred to as sequestration whereas stratigraphic and/or structural trapping and hydrodynamic trapping can be termed storage. Sequestration, therefore, implies the tying up of C in a geologically-stable form whereas storage implies a potentially shorter-term method.

An aquifer that serves as a repository for CO_2 is one part of a structural and stratigraphic package present within a sedimentary basin. Migration by gravity and groundwater flow may cause supercritical CO_2 to encounter diverse geochemical environments, brine and groundwater chemistries, sandstone and shale compositions, lateral facies transitions, etc. In general, the deep aquifers that will be considered for C disposal will have saline waters or brines. Overlying confining beds (aquitards) must also be considered as a part of this potentially rich reaction environment, the stability of which is critical to long-term containment of CO_2. The environment of such a CO_2 repository would also span a range of depths for initial emplacement and subsequent migration, and therefore a range of pressures and temperatures that are of interest geochemically. Pressures may range from a few bars where CO_2 has migrated to near-surface environments to several hundreds of bars within the initial zone of emplacement of supercritical CO_2. Temperatures may range as high as 150–200 °C, depending on local and regional geothermal gradients. Within this environment, CO_2 will be in the supercritical state because its critical point lies at 30.98 °C and 73.8 bars (Span and Wagner, 1996). A material in the supercritical state is neither liquid nor gas and is sometimes called supercritical fluid (Lake, 1989).

The published literature has primarily focused on carbonate precipitation, assuming that limited geochemical reactions occur within saline aquifer storage scenarios. Simple numerical models have used the Darcy equation and Fick's law and assume that the only reaction involving CO_2 is dissolution of supercritical CO_2 in aqueous solution (Lindeberg, 1997). Residence times and escape mechanisms are based on gravity migration. Leakage is due to a combination of physical, not chemical, phenomena, including lateral migration and subsequent release through subvertical fractures and faults. More advanced numerical modeling couples groundwater and heat flow equations with multiphase flow of water and dissolved, gaseous, and supercritical CO_2 (McPherson and Cole, 2000). In a 1 ka simulation of CO_2 injection within the Powder River Basin, Wyoming, most of the supercritical CO_2 dissolves into the aqueous state within 750 a. No allowance is made for other geochemical interaction between supercritical CO_2 and the host aquifer, although the potential importance of the geochemistry is acknowledged (McPherson and Cole, 2000).

A few studies do examine reactions in host rock in response to addition of CO_2 under reservoir temperature and pressure conditions. In numerical geochemical modeling studies that incorporate kinetic rate laws (Perkins and Gunter, 1995; Gunter et al., 2000) and one study combining experiment and modeling (Gunter et al., 1997), dissolution of silicate minerals in a brine and precipitation of carbonate are reported. In the latter study, however, experiments consisted of month-long batch reactions at 105 °C and 90 bars in which no silicate dissolution textures or new major reaction products were observed. With few exceptions (i.e., Gunter et al., 1997; Kaszuba and Janecky, 2000; Kaszuba et al., 2001), there is no published experimental evaluation of geochemical reactions that occur within a supercritical CO_2–brine–aquifer system at reservoir temperature and pressure. Despite the knowledge that supercritical CO_2 markedly effects equilibria in a variety of organic (Lucien and Foster, 2000) and inorganic (Raymond, 2002) systems, no systematic geochemical studies evaluate the effect of multiphase H_2O–CO_2 fluids on mineral equilibria. Aspects of the problem have been addressed, such as phase equilibria in metacarbonate rocks (Bowers and Helgeson, 1983) and numerical models that maintain CO_2 as an equilibrium phase (Perkins and Gunter, 1995; Gunter et al., 1997). However, important questions remain unanswered. For example, although the stability of the containment interface is critical to sequestration and long-term storage, no evaluation of the potential geochemical interactions between multi-phase fluids and the overlying confining beds has been undertaken. In effect, the reactive behavior of supercritical CO_2 under relevant geologic conditions is largely unknown.

The purpose of this study is to determine the extent of fluid–rock reactions, in addition to carbonate mineral precipitation, that may occur in an experimental brine aquifer–aquitard system that simulates geologic storage and sequestration of CO_2. Evidence for fluid–rock reactions include reaction textures on minerals comprising the aquifer and/or the aquitard, precipitation of carbonate mineral, and changes in brine chemistry imposed by CO_2. Reservoir temperature and pressure conditions vary widely, approximately 50–200 °C and 20–1000 bars (Hurter and Pollack, 1996; Carter et al., 1998; Hitchon

et al., 1999; Bachu, 2000; Benson, 2000; Oldenburg et al., 2001). The relatively high temperature of 200 °C was selected for this study so that kinetic rates of silicate reactions would be maximized. A pressure of 200 bars was chosen for consistency with and accessibility for sequestration scenarios.

All 3 lines of evidence for fluid–rock reactions were observed in the experiments, indicating that reactions among brines, carbonate and silicates are intimately coupled and not as simple as has been depicted in the C sequestration literature. A number of clear implications can be drawn from this exploratory investigation for reservoir C sequestration. The discussion is also extended to other systems in which supercritical CO_2 may have impact.

2. Material and methods

2.1. Experimental approach

A model aquifer-aquitard geochemical system was reacted with brine at 200 °C and 200 bars for 59 days (1413 h) to approach steady state. Carbon dioxide was then injected into the system and the experiment continued for another 80 days (1924 h). At 200 °C and 200 bars, CO_2 in the reaction cell is a supercritical fluid (Span and Wagner, 1996; Shyu et al., 1997) that is free to react with the aquifer–aquitard–brine system. The brine was periodically sampled and analyzed during the experiment. After the experiment was terminated, the solids and quenched brine were analyzed.

2.2. Experimental apparatus

The experiment was conducted in a flexible cell hydrothermal apparatus consisting of a Au–Ti reaction cell contained within a steel pressure vessel (Seyfried et al., 1987). The cell is plumbed to a valved capillary tube that serves as a sampling port. This equipment allows fluid samples to be withdrawn from the Au reaction cell at the temperature and pressure of an experiment and to be rapidly cooled to ambient conditions in less than a few seconds. Consequently, retrograde reactions with minerals that may occur during a prolonged quench process are avoided and solution composition can be analyzed along a reaction pathway. Fluids such as CO_2 can also be introduced into the reaction cell during an experiment to allow external modification of the fluid composition. This equipment also allows external control and monitoring of pressure and temperature.

2.3. Materials

Arkose was chosen as the geochemical and mineralogical representation of an aquifer for these experiments because it provides a diverse geochemical reaction basis and commonly occurs as the reservoir host in sedimentary basins. The arkose was constructed from equal amounts of naturally-occurring Minas Gerais quartz, oligoclase ($An_{17–21}$), and microcline ($Or_{91–97}$) exhibiting perthitic exsolution ($Or_{3–9}$). The quartz and oligoclase grains are angular mineral fragments that range in size from 1 to 5 mm. Microcline is also angular but is smaller in size, ranging from approximately 0.5 to 1 mm. Fracture edges on the quartz are sharp and chonchoidal fractures are well developed. The quartz is clear and contains no obvious Fe or Ti oxide inclusions. Oligoclase displays textures consistent with an igneous petrogenesis, including sieved cores, fritted zones surrounding the cores, and glassy inclusions. Biotite was added as a proxy for ferromagnesium minerals that occur in arkoses. Biotite grains range in size from approximately 0.1 to 1 mm.

A sample from the Silurian Maplewood Shale, an argillaceous shale from Monroe County, New York, USA, was selected as a geochemical representation of an aquitard. The shale is specimen #52 from the Ward's collection of North American Rocks (Ward's Natural Science Establishment, 1970). The shale contains "subordinate silty quartz grains, feldspar pieces, sericite flakes, calcite rhombs, and a few particles of pyrite, zircon, magnetite, and leucoxene in a dark matrix composed mainly of an illitic clay mineral" (Ward's Natural Science Establishment, 1970). Examination of the shale using optical and scanning electron microscopy and X-ray diffraction verified the abundance of clay minerals and quartz (65 and 27 vol.%, respectively) and revealed a subparallel alignment to the clays. The shale is also porous and contains framboidal pyrite, but no calcite was observed. For use in the experiment, the shale was broken into angular fragments approximately 0.5 to 1.5 cm in largest dimension.

The chemistry of the brine (Table 1) was modeled after saline aquifer compositions occurring in the Delaware Basin of southeastern New Mexico (Stein and Krumhansl, 1988) and synthesized using standard laboratory-grade salts. Sodium, Mg and K are the predominant cations and Cl^- the predominant anion. The ionic strength of the brine is 5.5 molal. Selection of a brine with relatively high Mg and Ca content allows examination of both precipitation of carbonate minerals from the brine and silicate reaction processes in this initial experimental investigation.

The experimental system was loaded with 3.3 g of arkose (1:1:1:0.3 quartz:plagioclase:microcline:biotite), 2.7 g of Maplewood Shale chips, and 90 g of brine. Following extraction of 24.4 g of brine as samples during the initial 1413 h of reactions, approximately 5 g of CO_2 followed by 2.1 g of fresh brine was injected into the reaction cell. Thus, the initial brine to rock mass ratio was 15.5:1 and the initial brine to CO_2 mass ratio was approximately 13.5:1.

Table 1
Water chemistry (in millimole/kg)

Time (h)	pH[a]	Na	K	Ca	Mg	Cl	Br	SO_4	SiO_2	Al	Fe	Mn	B	Charge imbalance meq (%)
Initial brine	7.15	1927	752	15.6	1403	5659	4.98	46.2	0.38				23.9	−168 (−3)
502		1618	586	16.8	1123	4679	4.44	39.8			2.11	0.189	31.5	−181 (−4)
670	4.73	1892	629	20.0	1172	4683	4.84	44.4	3.56	0.07	1.71	0.114	23.4	217 (4)
1005	4.70	1931	611	20.5	1185	4612	4.89	45.9	3.14	0.05	1.40	0.120	24.2	332 (7)
1412	4.86	1892	611[b]	20.5	1185[b]	4612[b]	4.84	48.7	3.32	0.18	0.71	0.099	23.6	285 (6)
CO_2 inject														
1413														
1487	5.33	2251	831	30.2	1634	5777	5.36	45.0			0.50	0.146	35.2	633 (10)
2013	5.63	1679	675	18.5	1279	5346	4.64	44.7	3.92	0.12	1.99	0.091	21.1	−407 (−8)
3335	5.61	1644	639	17.6	1201	5300	3.97	40.9	3.56	0.13	4.57	0.115	20.5	−579 (−12)
Quench														
3337	5.76	1605	637	16.9	1201	4557	3.94	39.7			3.85	0.106	22.2	112 (2)
Maximum 2σ uncertainty[c] (%)	4	3	3	3	3	5	5	5	5	30	3	3	3	

[a] pH reported is stable value measured on sample brine at standard temperature (25 °C) and at least partially degassed.
[b] Estimated concentrations.
[c] Maximum 2σ uncertainty is a combination of analytical uncertainty and uncertainty in sampling methods.

2.4. Analytical methods

Hydrothermal fluids within the reaction cell were sampled as described by Seyfried et al. (1987). Dissolved Si, Ca, Mg, Na, K and B were determined by ICP-ES, dissolved Al, Fe and Mn by ICP-MS, and dissolved anions by ion chromatography. Analytical precision of analyses is reported in Table 1. Solids were analyzed using optical microscopy, scanning electron microscopy (SEM), and X-ray diffraction (XRD). Samples analyzed with the SEM were mounted on 1-inch (25.4 mm) round C planchets using C sticky tabs and coated with approximately 200 Å of C. Secondary and backscattered electron signals and qualitative X-Ray analysis using Energy Dispersive Spectrometry (EDS) were used. The accelerating potential was 20 kV with beam current dependent on application.

Charge imbalance in analyses of samples collected at 1412 and 1487 h presented some difficulties for the brine chemistry data set. The authors suspect that these problems result from evaporative losses due to the interval of time between collection and analysis and improper sample handling, respectively. For the 1487-h sample, the matter was resolved by re-analyzing several dilution aliquots and careful evaluation of the data. This process resulted in a charge imbalance of approximately 10%. The 1412-h sample is more problematic. An insufficient amount of brine solution was left to re-analyze the sample. The problem appears to be in the Cl^-, Mg and K analyses, which are significantly different from the previous sample.

3. Results

3.1. Reaction of solid phases

Each of the minerals in the arkose displays some evidence of participating in fluid-rock reactions. Although the edges of quartz grains used as starting material have some angular pits, those observed in quartz from the experiment are more numerous and distinctly rounded and enlarged (Fig. 1). Abundant clay mineral grains adhere to quartz from the experiment and commonly stretch across edges of pits and open fractures. Potassic lamellae in perthitic microcline are etched relative to sodic lamallae by the experimental reactions (Fig. 2). Development of etch pits in the initially smooth fracture surfaces is accompanied by formation of relatively large patches of clays.

Clay minerals (smectite) are present in abundance on oligoclase surfaces and cleavages (Fig. 3), whereas oligoclase starting material is largely free of clay minerals. Wispy clay minerals commonly fill and stretch across open cleavages. Unlike microcline, however, no differential etching of the oligoclase surface is observed. Some biotite is coated with a mat of small (<5 μm) magnesite rosettes intergrown with clay minerals (smectite) (Fig. 4), particularly along the edges. Biotite is also bleached and rounded along the edges, even on sheets without the magnesite coating. In contrast, biotite in the starting material is fresh looking and the edges of biotite sheets are angular.

The shale shows several textures indicative of participation in fluid–rock reactions (Fig. 5). On several shale fragments, the edges are lighter relative to the starting

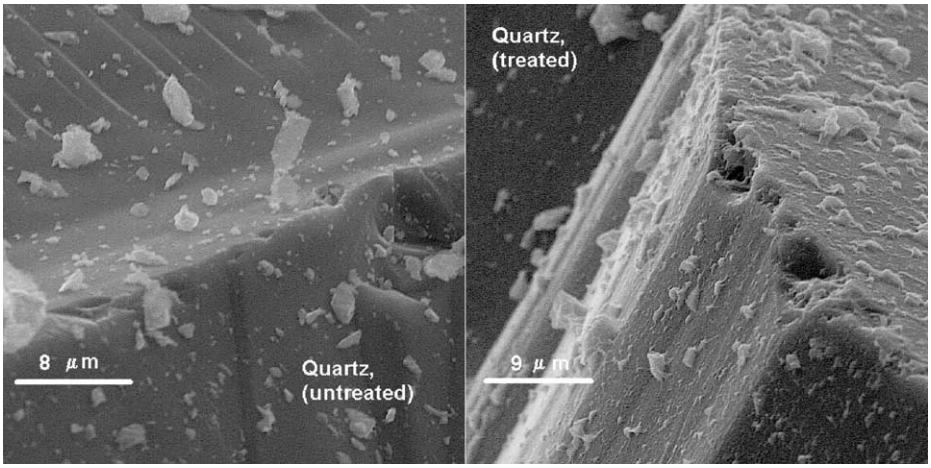

Fig. 1. Secondary electron SEM micrographs of quartz. The edges of quartz grains in the starting material contain pits that are angular (image at left). Pits in quartz from the experiment are more numerous and distinctly rounded and enlarged (image at right).

material. Wispy clay coatings drape across surfaces and small cavities in the shale. The euhedral form of constituent minerals and the number and size of cavities and pores have either diminished or are obscured by the clays. Patchy accumulations of subhedral halite crystals are present on the shale surfaces, possibly due to trapping of brine on the shale during quench and subsequent processing of the experimental solids.

Magnesite is present in two distinct size fractions of euhedral crystals: large (100 μm and greater) bladed crystals that occur as discrete rosettes visible to the naked eye (Fig. 6) and small (<5 μm) crystals that coat biotite (Fig. 4). X-ray diffraction of the large rosettes confirms that the mineral is magnesite.

Analcime trapezohedrons are ubiquitous in the experiment (Fig. 7). They occur both as large connected masses of crystalline aggregates and as single crystals lodged in fractures and cleavages of other materials. Analcime crystals in the large masses display a rounded, skeletal habit and are coated with smectite, kaolinite and mica. X-ray diffraction confirms the identity of analcime and the coatings. The nature of the skeletal habit, whether from rapid crystallization or because analcime became unstable in the CO_2-bearing system, is not clear from this study.

3.2. Brine chemistry during reaction

The major ions in the brine, including Na, K, Mg, Ca, Cl, SiO_2, B, and the pH, stabilized within approximately 670 h after beginning the experiment (Table 1, Figs. 8 and 9). Stable concentrations of Na and B are approximately equal to the concentrations initially present in the brine. Potassium, Mg and Cl decreased by 15–20% in this same interval, and Ca increased by approximately 30%. Silica, not present in the initial brine, also stabilized in this interval at slightly below calculated quartz solubility concentrations. In contrast, SO_4 and Fe concentrations continued to drift with time. After an initial decrease in concentration, SO_4 increased with time. After an initial spike in concentration, Fe decreases with time, during the brine reaction with the minerals. Manganese and Al display no coherent trends, as both occur at relatively low concentrations in the brine. The stabilization of major ion chemistry in the brine suggests that the brine achieved an approximate steady state, controlled by the alteration mineral assemblage. The decrease in Cl is not understood but may be due to Cl^-–OH^- exchange reactions in the sheet silicates.

Injection of approximately 5 g of CO_2 into the reaction cell at 1413 h resulted in an increase in the pressure

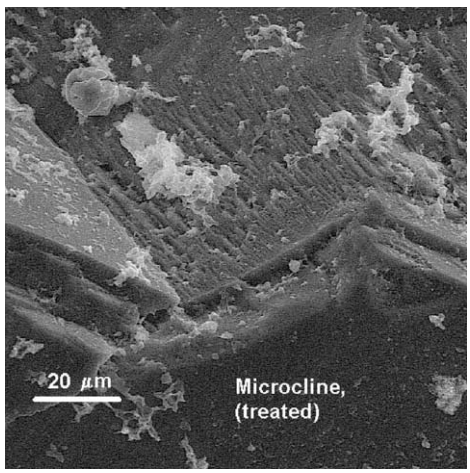

Fig. 2. Secondary electron SEM micrograph of perthitic microcline. Potassic lamellae are etched relative to sodic lamallae, a texture not present in the starting material.

of the experimental system from 200 bars to 230 bars. After manual adjustment to 200 bars, the pressure decreased by a total of 26 bars over the course of the following 72 h (Fig. 10). The system pressure subsequently stabilized, with fluctuations of only a few bars that were correlated to ambient temperature changes in the laboratory and experimental apparatus. The 26 bar pressure decrease is consistent with behavior observed previously in brine–MgO–CO_2 experiments (Kaszuba and Janecky, 2000; Kaszuba et al., 2001).

Concentrations of Na, K, Cl, Mg, Ca and B in the CO_2-bearing system increased by approximately 20–50% relative to conditions observed in the initial brine system, as measured in the sampling event held 72 h after injection of CO_2 (Table 1, Fig. 8). The pH measured in partially degassed brine at 25 °C also increased from approximately 4.7 to 5.6 (Fig. 9). In contrast, the pH calculated for brine saturated with CO_2 at temperature decreased to approximately 3.4. Concentrations of Br increased by approximately 11% in this same interval, Fe and SO_4 both decreased, and Mn increased. Aluminium and SiO_2 were not analyzed in this sample. It is possible that SiO_2 also increased, because the subsequent concentrations are higher than before CO_2 injection and the observed trend in the CO_2-bearing system is decreasing. A portion of the increase in concentration of the major ions is due to experimental procedure. In the experiment, a small aliquot of brine was injected following addition of CO_2 to ensure that all CO_2 was introduced into the reaction cell. It is

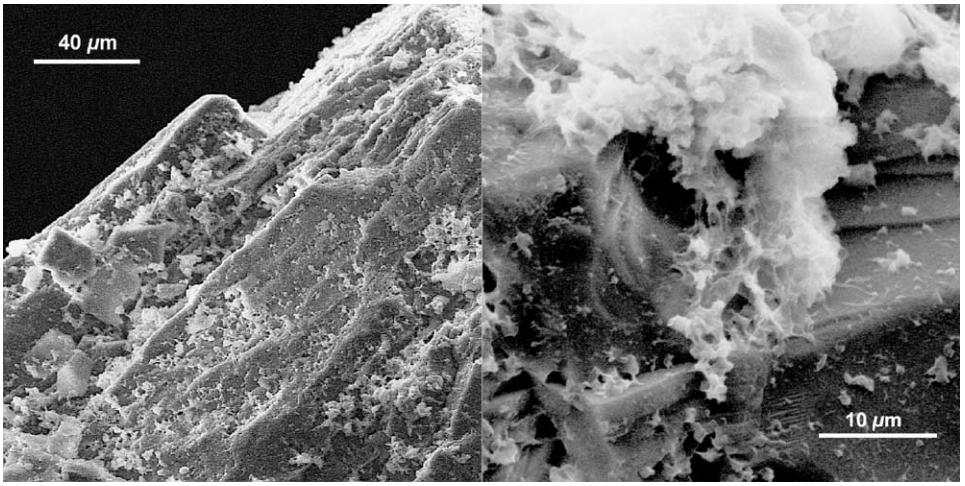

Fig. 3. Secondary electron SEM micrograph of oligoclase. Clay minerals are present in abundance on plagioclase surfaces, a texture not present in the starting material.

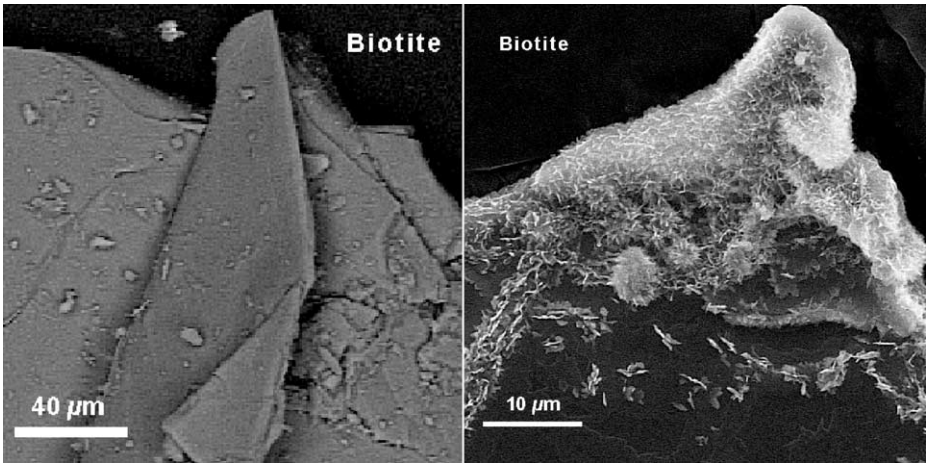

Fig. 4. SEM micrographs of biotite. Biotite in the starting material (backscatter electron image at left) is fresh looking and the edges of biotite sheets are angular. Biotite from the experiment (secondary electron image at right) is coated with a mat of small (<5 μm) magnesite rosettes intergrown with clay minerals, particularly along the edge that is somewhat rounded.

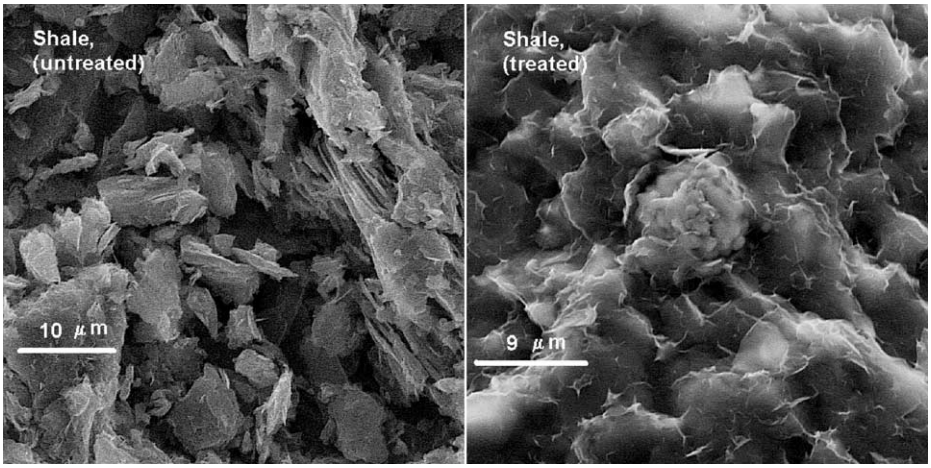

Fig. 5. Secondary electron SEM micrographs of shale starting material (image at left) and shale from the experiment (image at right). The euhedral form of constituent minerals has diminished and the number and size of pores has decreased in the shale from the experiment.

estimated that this procedure contributed a maximum of 10% to the Cl^- increase reported in Table 1, and less for the other major ions. The significant increase in concentration of the major ions, therefore, suggests the rock dissolved by reaction with CO_2 and brine, behavior consistent with the calculated drop in pH at temperature due to CO_2 injection (Fig. 9). The pressure drop observed in the reaction system (Fig. 10), therefore, appears to be an external measure of the overall brine–CO_2–rock reaction rate for this process. Instrumentation to measure CO_2 dissolved in brine samples from the reaction cell was not available during this experiment. However, exsolved gas captured with brine in the sampling syringes (assumed to be predominantly CO_2) was greatly increased following injection of CO_2 into the reaction cell.

The CO_2–brine–arkose–shale system reached an approximate steady state by 2000 h, 1330 h after injection of the CO_2 (Fig. 8, Table 1). The resulting brine composition is, moreover, significantly different than in the CO_2-undersaturated system. Concentrations of Na, Ca and B are approximately 12% lower, Mg and K are approximately 5% greater, Cl is 16% greater, and calculated pH has decreased by 1.3 pH units (Fig. 9). Steady state Br and SO_4 concentrations are not observed. In general, however, Br concentrations in the CO_2-bearing system are lower than in the CO_2-undersaturated system. Also, SO_4 concentrations in the CO_2-bearing system are generally lower and decreasing, in contrast to the CO_2-undersaturated system with generally higher SO_4 concentrations that increased with time. Iron concentration trend is again inverse to SO_4, increasing with time in the CO_2-bearing system in contrast to the CO_2-undersaturated system. Silica concentrations continue to trend downwards with time, but are at least 10% higher than before CO_2 injection.

The sample of brine that was collected after the experiment was quenched displays a significant change in Cl^- concentration relative to the sample collected at 200 °C and 200 bars (Table 1 and Fig. 8). Chloride concentration decreases to a level equal to initial brine reaction steady state concentrations. No other single major element displays this relationship to the same magnitude as Cl^-, although B concentrations increase (by approximately 8%) and Fe concentrations decrease (by approximately 16%) towards pre-injection levels. The behavior of Cl^- suggests that its concentration in brine could be controlled by fluid–fluid processes in addition to mineral–fluid equilibria, as discussed in the following section. The behavior of B, Ca, Na, Br and

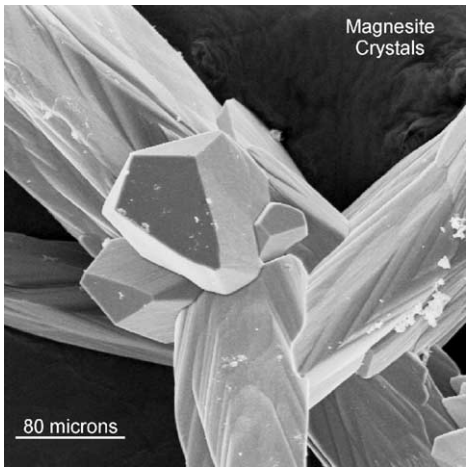

Fig. 6. Secondary electron SEM micrograph of a magnesite rosette. Large (> 100 μm), euhedral crystals such as these precipitated in the experiment after CO_2 was added.

SO_4 is consistent with removal of these components from the brine by precipitation of solids. In contrast, Fe, Mg and K behavior is consistent with mineral dissolution during quench. These collective changes in brine chemistry suggest other potential complexities in CO_2 reactions with the brine-rock system.

4. Discussion

4.1. Fluid–rock reactions and processes

In agreement with models proposed for geologic sequestration of C (e.g., Gunter et al., 2000), addition of supercritical CO_2 into an experimental brine aquifer system precipitated mineral carbonate(s). The pressure decrease following injection of CO_2 is indicative of a decrease in the volume of the system due to the phase change of supercritical CO_2, to dissolved carbonate, to mineral carbonate. In addition to carbonate precipitation, however, a diversity of other fluid-rock reactions takes place within the experimental system. Silicate minerals in the arkose and the shale display textures indicating that these phases are reacting strongly with the fluid. The brine chemistry changed with addition of supercritical CO_2, as manifest by the large changes in elemental abundances within 72 h of addition of the CO_2. These initial changes dissipated as time elapsed, yielding steady state conditions that exhibit elemental abundances different from the CO_2-undersaturated system.

The mineral assemblage present at the conclusion of the experiment, analcime + smectite + quartz, indicates zeolite facies metamorphic conditions. The absence of albite + white mica + prehnite + pumpellyite indicates that prehnite–pumpellyite facies stability was not achieved. The significance of skeletal analcime is unclear. This texture may represent rapid analcime crystallization, or it may be a texture-related reaction resulting from the presence and/or addition of supercritical CO_2.

In addition to reactions during the run of the experiment, additional changes occurred as a result of quenching from 200 °C and 200 bars to 25 °C and 1 bar. Of particular interest, Cl^- in the quenched brine sample decreased from the steady state concentrations existing with brine and supercritical CO_2 to the same concentrations observed in the CO_2-undersaturated system. In the absence of precipitation of Cl^--bearing minerals (e.g. simple salts or Cl^--bearing silicates such as scapolite), it is valuable to examine reactions involving fluid chemistry that could control such Cl^- behavior. Inspection of the isothermic (200 °C) phase diagram for H_2O + CO_2 (Fig. 11) indicates that the composition of fluids will not be simple end-members. Instead, two fluids, one rich in H_2O and a second rich in CO_2, will co-exist at 200 °C and 200 bars. The H_2O-rich fluid contains a small fraction of CO_2, whereas the CO_2-rich fluid contains approximately 15 mol% H_2O. Therefore, supercritical CO_2 addition can desiccate the brine solution at conditions of the experimental reactions of 200 °C and 200 bars, enriching the remaining brine in Cl^-. Desiccation is one likely cause of the Cl^- enrichment observed in the experiment following injection of CO_2. At 25 °C and 1 bar, the supercritical CO_2-rich fluid becomes a gas and previously dissolved H_2O will be released back into the brine. Chloride concentrations

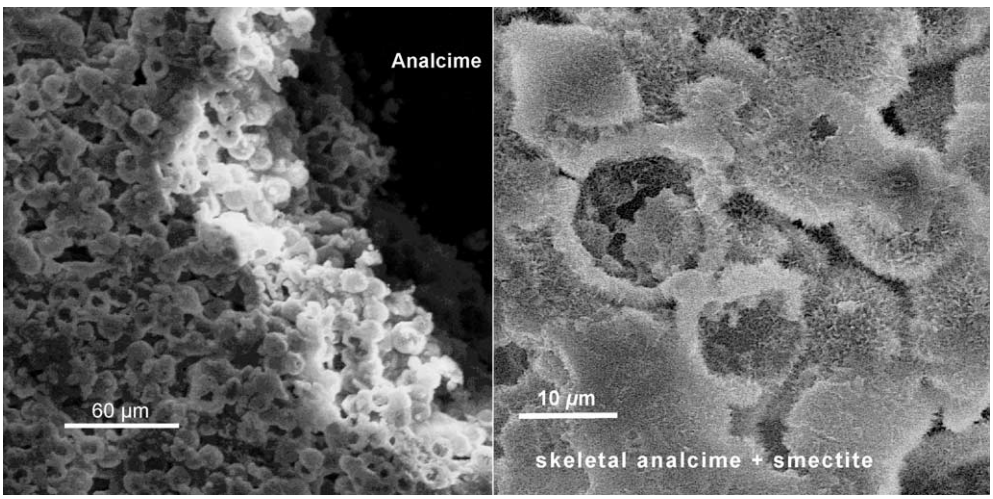

Fig. 7. Secondary electron SEM micrographs of analcime trapezohedrons precipitated in the experiment. The close-up image on the right displays the skeletal habit and smectite (plus kaolinite and mica) coating that is common to much of the analcime. The process controlling development of the skeletal habit is not clear from this study.

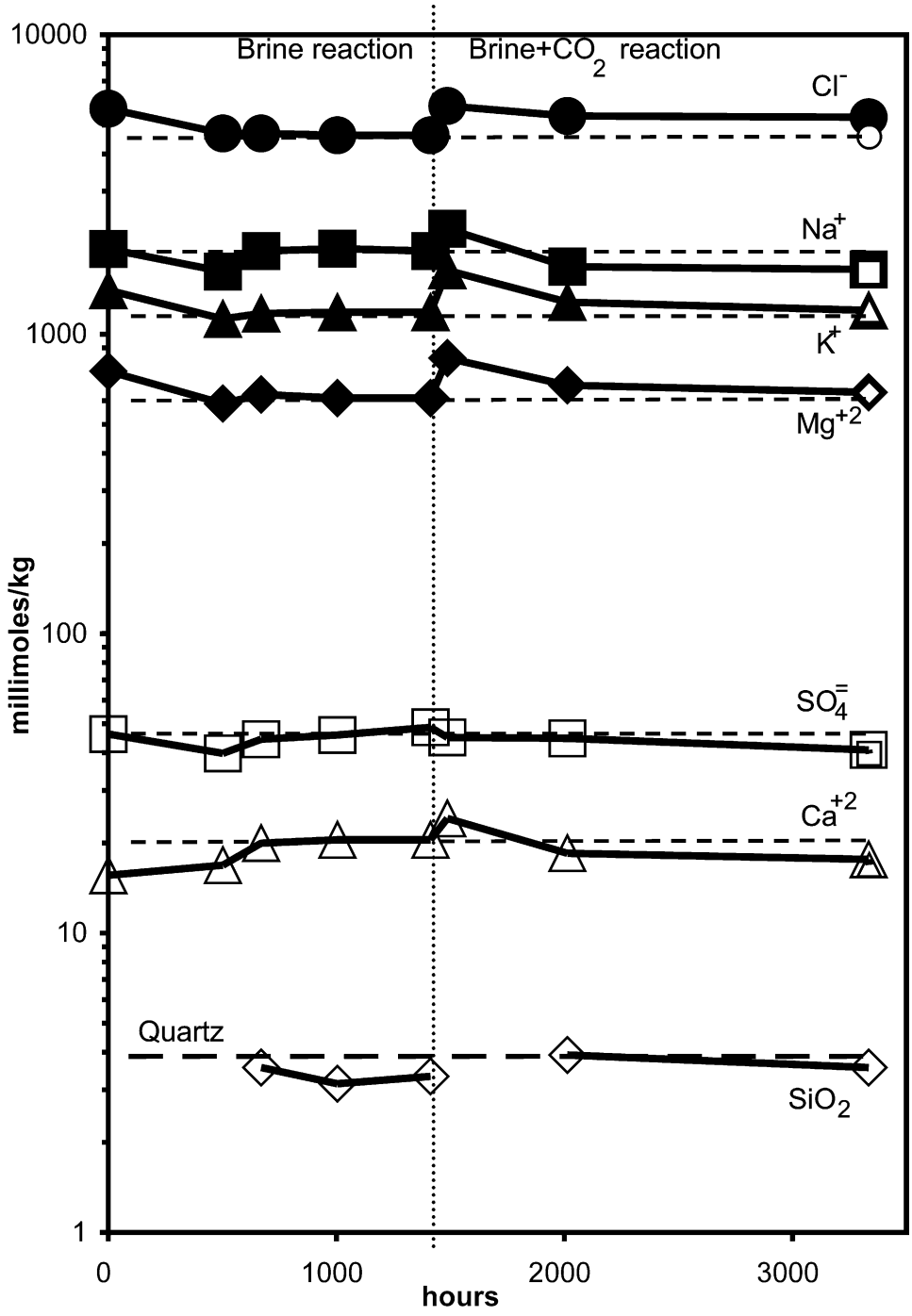

Fig. 8. Brine chemistry as a function of time during the experimental reaction for Cl (solid circles), Na (solid squares), K (solid triangles), Mg (solid diamonds), SO_4 (squares), Ca (triangles), and SiO_2 (diamonds). Dashed lines represent approximate stable concentrations attained during the brine-rock reaction, with the exception of SiO_2, which is compared to calculated quartz solubility. Carbon dioxide was injected into the reaction cell at 1413 h ($\sim$5 g CO_2 plus 2.1 g brine into $\sim$65.6 g brine) to produce a fluid to rock ratio of $\sim$66/5/6 for brine/CO_2/minerals. A two-phase fluid (brine + supercritical CO_2) was also formed. Uncertainties are smaller than the size of the symbols. Quenched experiment samples are represented by smaller symbols.

thereby can be diluted to return to their approximate initial state (neglecting the removal of small amounts of brine as samples during the experiment).

Is such a multi-phase fluid reaction process a reasonable or well-constrained interpretation in this experiment? In addition to the observations from the quench sample, the interpretation above for system pressure behavior, that supercritical CO_2 injected into the cell reacts and then stabilizes, is generally consistent with the high Cl^- in the 1487 h sample and the concentration observed in the final two samples (Fig. 8 and Table 1). There are aspects of the basic data which are not well enough constrained to be definitive. Most importantly, the phase diagram in Fig. 11 was developed for pure H_2O and CO_2 at 200 °C. The brine composition will change the activity of H_2O and therefore can result in significant changes to the solubility of H_2O in the CO_2-rich phase, with the expectation that the general form of the phase diagram will remain. The authors have made rough calculations of the relative mass balances for H_2O and Cl in this experiment, using data from Fig. 11. These calculations indicate that, for the relative amounts of brine and CO_2 in this experiment, the resulting changes in Cl^- concentration in the brine phase would be much smaller than observed. Alternatively, the experiments could indicate a much greater H_2O solubility in the CO_2-rich phase. This discussion does point out that a major requirement for evaluating and modeling C sequestration processes and consequences in brine-containing reservoir systems will be a substantial enhancement of characterization of brine–CO_2 phase behavior and mixed phase compositional controls. Simultaneously, further work must experimentally confirm that reactions between the mineral and fluid phases are not involved as well, even though they could not be identified directly in solid products from this experiment.

4.2. Implications for carbon management

In addition to dissolution of supercritical CO_2, carbonate precipitation, and a drop in pH, this study confirms that the following geochemical reactions and processes may also take place (Fig. 12):

1. Reactions at the interface between two phase fluid systems (supercritical CO_2 and brine) and the aquifer minerals (in addition to those which produce cements and plug pores),
2. Reactions at the interface between two phase fluid systems (supercritical CO_2 and brine) and the aquitard minerals, and
3. Desiccation of the brine by extraction of water into the injected supercritical CO_2.

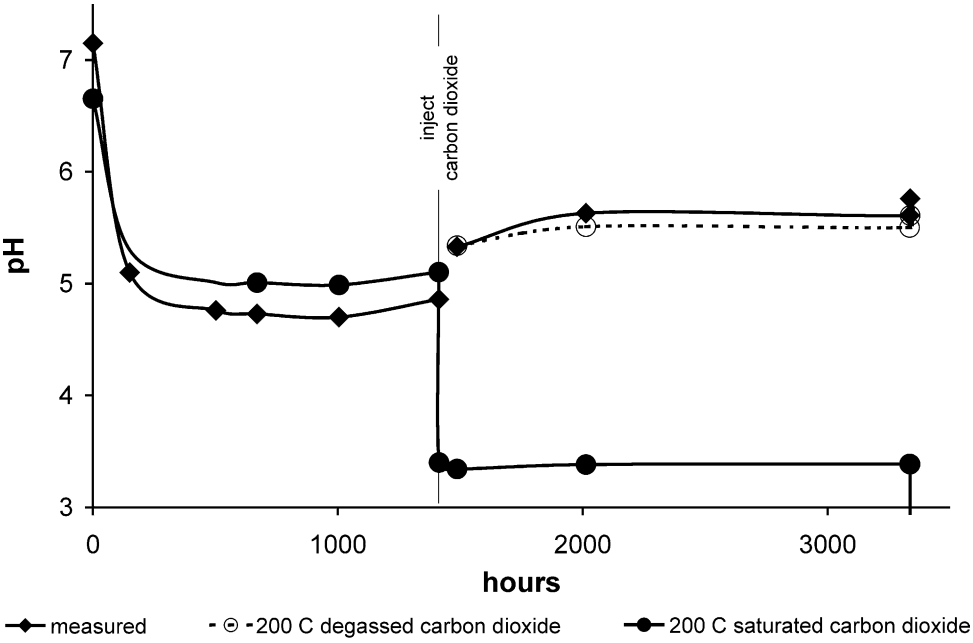

Fig. 9. Interpretation of pH behavior during experiment. The brine interaction with the minerals at 200 °C and 200 bars results in a measured pH decrease to approximately 4.7 (diamonds). This initial pH decrease could go below 4.7 if brine reactions are faster than silicate mineral dissolution (Seyfried, 1977; Janecky, 1982). Injection of CO_2 is accompanied by a measured pH increase to approximately 5.6 in samples that were cooled to 25 °C and at least partially degassed. Calculation of speciation using EQ3/6 and the b-dot ion association model (Wolery, 1992) for CO_2-saturated brine samples at 200 °C indicates an in situ pH of approximately 3.4 (solid circles).

Reactions among supercritical CO_2, the in-place brine, the aquifer and the aquitard may give rise to a number of consequences of geochemical and geotechnical significance. This experiment has demonstrated that a complex suite of reactions occurs on a measurable time scale, with important changes in brine pH and other chemistry. Reactions in the aquitard that exhibit negative volume changes may produce high permeability channels, concomitant loss of integrity of the system, and subsequent release of CO_2. Alternatively, reactions in the aquitard may yield mineral assemblages that fill porosity and decrease permeability due to positive volume change or transport of reactive components from the aquifer into the aquitard as observed in this experiment (Fig. 5). In addition to the potentially positive aspects of porosity decreases, such changes may result in enhanced brittle character relative to predecessor mineral assemblages, and consequent failure modes. Competency contrasts may develop between a carapace of reacted material overlying supercritical CO_2 containing zones and the unreacted periphery of the aquitard. Fracturing, loss of system integrity, and movement of CO_2 may result. Reactions that exhibit positive volume changes and reactive chemical transport may, in other cases, produce self-healing fractures. These scenarios are consistent with the results of this study and illustrate the richness of geochemical complexities previously unexamined. The feasibility for development of a successful CO_2 repository, including even a repository that can be designed or optimized with the capacity to self heal fractures, must account for these potential reactions.

Desiccation of the brine by supercritical CO_2 can introduce additional complications for a CO_2 repository. Dessication will produce density contrasts within the brine that could lead to gravitational instability and vertical components of flow. Chemical fractionation of brine within the saline aquifer is also possible, with geochemical reaction implications. Brine desiccation also suggests the potential for establishing localized

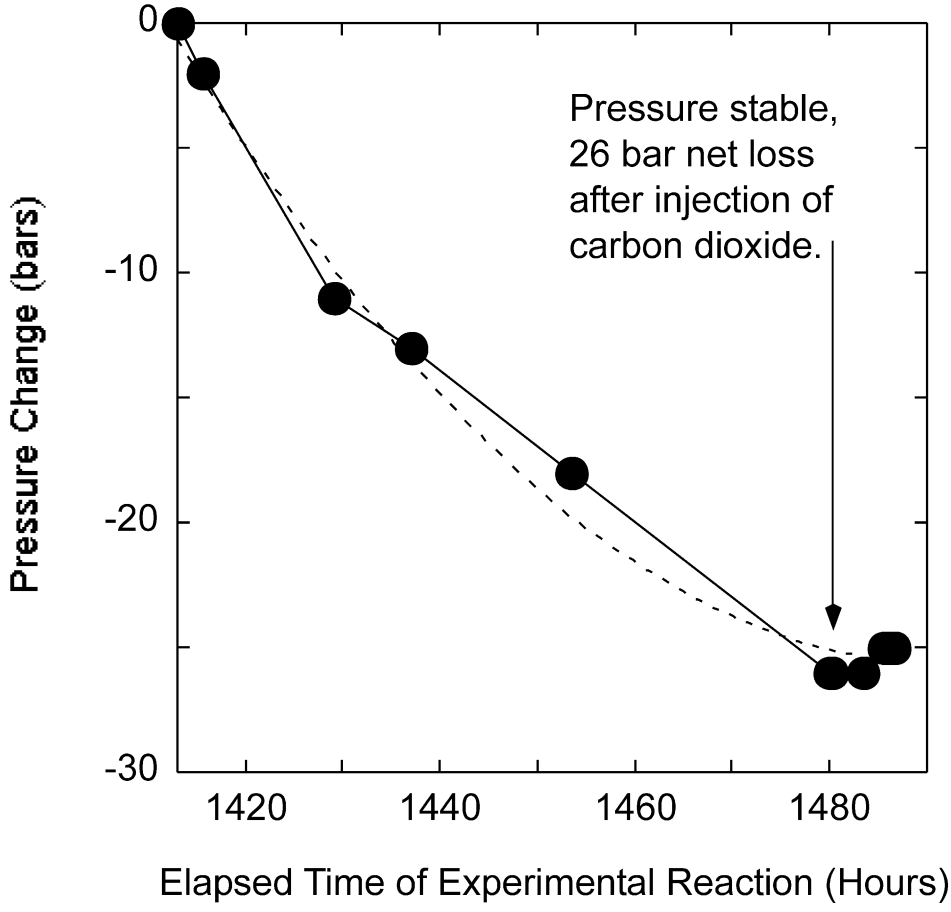

Fig. 10. Change in system pressure following injection of supercritical CO_2 into the reaction cell at 1413 h. Relative uncertainty is less than 2 bars. The pressure loss is interpreted as initial reaction with injected CO_2 and consequent consumption of supercritical CO_2 fluid until a relatively stable state is achieved at approximately 1480 h. The dashed line is a polynomial curve fit to the data.

micro-environments of high ionic strength at the interface between supercritical CO_2 and the brine aquifer. Fluid–rock reactions at these interfaces may differ from reactions in the bulk system. The direct effects of desiccation processes on the stability of a stored mass of supercritical CO_2 are uncertain. Will formation of a higher density brine boundary layer result in focusing flow of the CO_2-rich phase or impede its spread? What are the implications for fingering, mixing and carbonate mineral precipitation? Further experiments and system-scale modeling leading to investigation of a field scale system are needed to understand these effects. It also must be kept in mind that fluid-rock reactions at these interfaces may differ from reactions in the bulk system, even more strongly than found in this experiment.

In addition to the large-scale influences on C sequestration in reservoirs, these local scale geochemical processes may provide important characteristics for monitoring and evaluation. Geophysical techniques for evaluating the success of a CO_2 repository could take advantage of the process of brine desiccation by imaging density and electrical property contrasts. Chloride and other elements that exhibit behavior dominated by H_2O + CO_2 phase equilibria could also be monitored as geochemical indicators in interconnected or deep-seated aquifers, springs, or water wells. Changes in concentrations of these elements may provide clues to the subsurface disposition of stored CO_2. This approach may also provide new perspectives for evaluating the dynamics of existing reservoirs containing supercritical CO_2.

At a minimum, this experimental study demonstrates that systems for geologic sequestration of carbon have potential for geochemical reactions that extend beyond

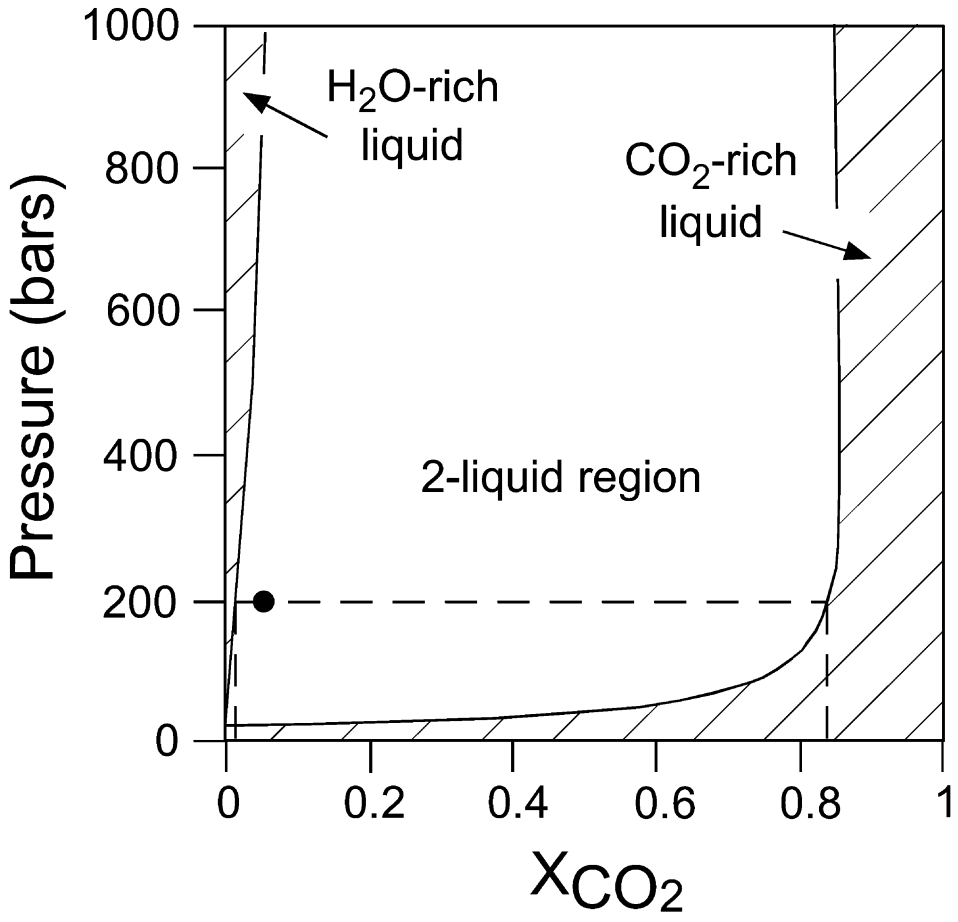

Fig. 11. Pressure-X_{CO_2} phase diagram for H_2O + CO_2 at 200 °C (Shyu et al., 1997). The regions of H_2O-rich and CO_2-rich liquid, with intervening immiscible two-liquid region, are shown. The solid dot represents the approximate composition of this experimental system after injection of CO_2, and the dashed line represents the phase relationships specific to this composition. While differences exist among the experimental data for the CO_2-rich side of the diagram, where reported compositions differ by as much as 15 mol% [compare data of Malinin (1959) and Todheide and Franck (1963) to Takenouchi and Kennedy (1964)], the general relationships are in broad agreement.

simple aqueous dissolution of CO_2 and precipitation of carbonate minerals. This simple conclusion is consistent with modeling predictions (Perkins and Gunter, 1995; Gunter et al., 1997, 2000) and adds another dimension of complexity and opportunity that must be understood if large amounts of supercritical CO_2 are to be successfully sequestered or stored in many different reservoirs.

4.3. Carbonate cements

Although calcite is one of the most common cements in sandstone, calcite cementation processes in sandstone are not well understood. Considerable spatial and chemical heterogeneity of calcite cement exists on a wide range of scales, from thin section to outcrop (to sedimentary basin?) (e.g. McBride et al., 1995; Milliken, 2001, and references therein). The source(s) of carbonate, the mechanisms of transport and precipitation, and the processes that produce heterogeneous distributions of carbonate cements have been explained in a variety of ways. Explanations that feature or combine differential flow paths, accumulations of shell-rich layers, detrital carbonate, diffusion, advection, proximity to carbonate-bearing shales, and proximity to fractures and faults have all been invoked (McBride et al., 1995, and references therein). For example, mechanisms proposed for calcite cements in the Stevens Sandstone, San Joaquin basin, California, include large-scale mass transfer from deeper, hotter beds (Schultz et al., 1989), "seismic pumping events" leading to episodic injections of hot, calcite-saturated water from depth (Wood and Boles, 1991), and localized variability in CO_2 fugacity (Wilson et al., 2000). A comprehensive modeling study of fluid flow, mass transport, and diagenesis in the Stevens Sandstone concluded that plagioclase dissolution drove precipitation of calcite cement (Wilson et al., 2000). However, Wilson et al. (2000) acknowledge an important discrepancy between the maximum amount of calcite predicted in their models and the actual amount observed in core (0.7 and 1–1.5 vol.%, respectively). In

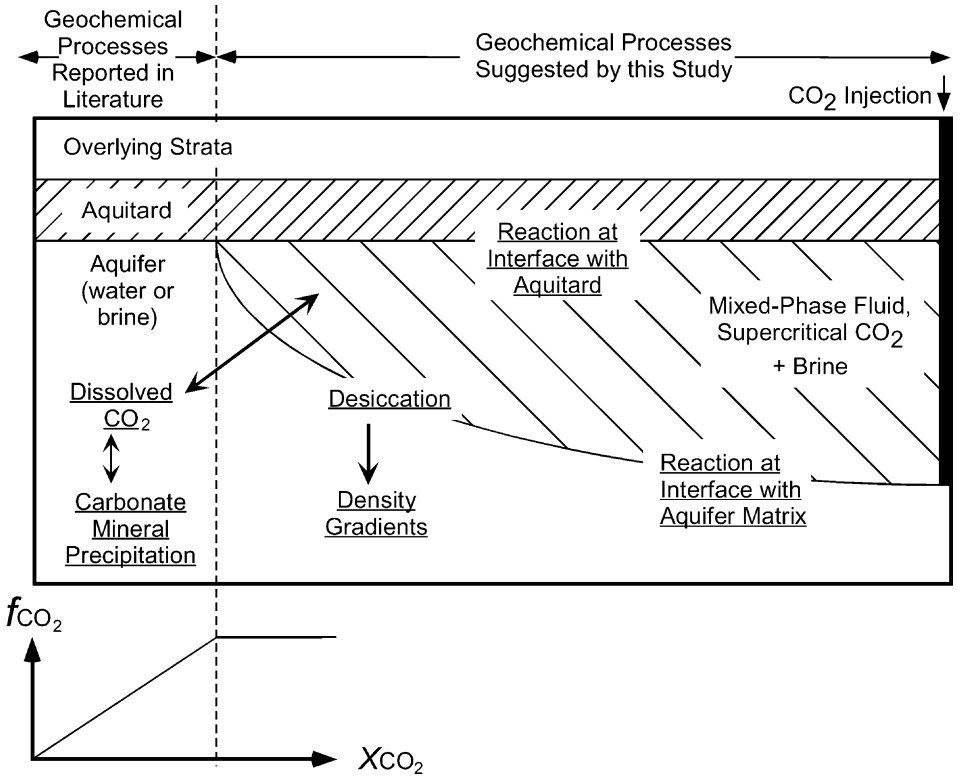

Fig. 12. Schematic vertical geologic cross-section representation of geochemical processes (underlined labels) that may occur as a result of emplacing supercritical CO_2 into a saline aquifer via injection (injection well at far right). Besides aqueous dissolution of supercritical CO_2 and precipitation of carbonate minerals, the work suggests that additional geochemical reactions will take place. Dissolution and precipitation may occur at the interface with the silicate-bearing aquifer and aquitard, and desiccation of the brine may produce density contrasts. The plot beneath the figure depicts the fugacity-mole fraction CO_2 relationships for the system. Presence of a supercritical CO_2 phase provides a reservoir of constant fugacity that is free to react with the adjacent geochemical environment.

addition, petrographic observations suggest that plagioclase dissolution and albitization began well after the onset of calcite cementation (Wilson et al., 2000).

In light of the present experimental work, it is suggested that multi-phase equilibrium relationships between supercritical CO_2 and aquifer–brine systems may be an important aspect in generation of the large amounts and heterogeneous distributions of calcite cement in some sandstones and veins. In the case of the Stevens Sandstone, the conditions under which calcite cement precipitated, greater than 300 bars at 45–105 °C for sporadic cementation events (Wood and Boles, 1991; Wilson et al., 2000), are consistent with the conditions at which CO_2 can exist in its supercritical state (greater than the pure CO_2 critical point of 31.1 °C and 73.8 bars). Simple mass balance calculations suggest that, between 50 °C and 200 °C, reaction of only a few pore volumes of supercritical CO_2 can produce 1 vol.% of calcite cement (Fig. 13). In contrast, approximately 10^7 pore volumes of carbonate-saturated aqueous fluid would be needed to produce an equivalent amount of calcite cement. Supercritical CO_2 would also provide a concentrated supply of carbonate that buffers the fugacity of aqueous carbonate.

Heterogeneous distribution of calcite cement is commonly described as random and without regard to the physical characteristics of grain size and porosity (e.g. Milliken, 2001, and references therein). Immiscibility between supercritical CO_2 and brines, as well as the substantial differences in transport properties (e.g. density differences between supercritical CO_2 + H_2O mixtures and pure H_2O (Blencoe et al., 2001) that are enhanced with decreasing temperature and pressure), may provide the explanation for at least some of these occurrences. As an example, the potential distribution of immiscible globules within a host supercritical fluid is analogous to the spatial arrangement of calcite-cemented concretions documented for some sandstones.

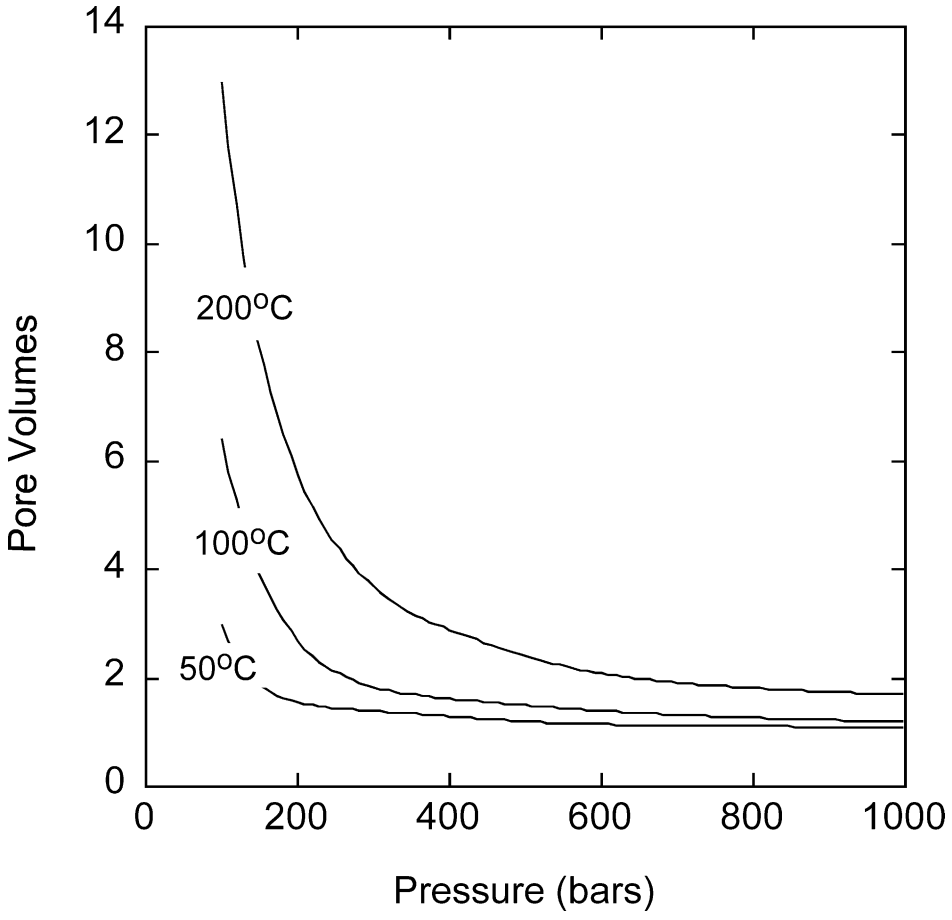

Fig. 13. Pore volumes of supercritical CO_2 needed to replace 1% of the porosity of sandstone with calcite. Curves were calculated by assuming that 100% of available CO_2 is converted to calcite and by using the density of supercritical CO_2 at pressure and temperature (Span and Wagner, 1996). Mole fraction of CO_2 at temperature and pressure are based on Shyu et al. (1997).

5. Summary and conclusions

This experimental investigation examines geochemical reactions and processes among supercritical CO_2, brine, and host rock at geologically-relevant pressure and temperature. It is the one of the first experimental studies to identify the potential for geochemical interaction among these phases in the largely-unexplored physical-chemical region between low-grade metamorphic environments, with CO_2 as a water-miscible fluid, and hydrologic environments containing gaseous and aqueous CO_2. The following are concluded from these experiments:

1. Supercritical CO_2 causes brine pH to decrease, validating assumptions and models about the effect of supercritical CO_2 on brine. The pH of quenched brine rebounds as CO_2-charged brine degasses.
2. Reaction among supercritical CO_2, brine, and rock exhibits relatively rapid kinetics that are similar to rates measured in systems containing little CO_2.
3. Transfer of H_2O from brine to supercritical CO_2 may have substantial and interesting consequences for mineral reactions and hydrodynamic stability.
4. Besides direct application to geologic sequestration of C, an understanding of multi-phase fluid equilibrium relationships between supercritical CO_2 and aquifer-brine systems raises new questions and potential interpretations in a wide variety of natural geologic systems. Since supercritical CO_2 is not directly observed or sampled in geologic systems, fluid inclusions (both primary and secondary) may be the only direct means of investigating reinterpretations of processes. In particular, multi-phase fluid equilibria may account for the large amounts and heterogeneous distributions of calcite cement in a wide variety of geologic systems, particularly in sedimentary basin sandstones.

Acknowledgements

Funding was provided by Los Alamos National Laboratory (LDRD/DR) for this research and by the US Department of Energy, Basic Energy Sciences, Geosciences Program for the hydrothermal laboratory facilities. Steve Chipera provided XRD analyses, Dale Counce, Kate Jones, and Laura Wolfsberg provided brine analyses, and Emily Kluk provided XRF analyses. Dr. W.D. Gunter provided a constructive and detailed review of the manuscript. JPK thanks DB for his guidance and mentorship. This manuscript is assigned LANL LAUR #01-6757.

References

Bachu, S., 2000. Sequestration of CO_2 in geological media: criteria and approach for site selection in response to climate change. Energy Convers. Mgmt. 41, 953–970.

Bachu, S., Gunter, W.D., Perkins, E.H., 1994. Aquifer disposal of CO_2: hydrodynamic and mineral trapping. Energy Convers. Mgmt. 35, 269–279.

Benson, S.M., 2000. Advances in geologic sequestration: identifying and addressing key issues. Geol. Soc. Am., Abstr. with Prog. 32, A200.

Bergman, P.D., Winter, E.M., Chen, Z.-Y., 1997. Disposal of power plant CO_2 in depleted oil and gas reservoirs in Texas. Energy Convers. Mgmt. 38 (SS), S211–S216.

Blencoe, J.G., Anovitz, L.M., Singh, J., Seitz, J.C., 2001. Relative buoyancies of CO_2-H_2O mixtures at 300-400 °C and presures to 100 megapascals. Geol. Soc. Am., Abstr. with Prog. 33, A17.

Bowers, T.S., Helgeson, H.C., 1983. Calculation of the thermodynamic and geochemical consequences of nonideal mixing in the system H_2O-CO_2-NaCl on phase-relations in geologic systems: metamorphic equilibria at high pressures and temperatures. Am. Mineral. 68, 1059–1075.

Carter, L.S., Kelley, S.A., Blackwell, D.D., Naeser, N.D., 1998. Heat flow and thermal history of the Anadarko basin, Oklahoma. AAPG Bull. 82, 291–316.

Freund, P., Ormerod, W.G., 1997. Progress toward storage of carbon dioxide. Energy Convers. Mgmt. 38 (SS), S199–S204.

Gunter, W.D., Perkins, E.H., Hutcheon, I., 2000. Aquifer disposal of acid gases: modelling of water-rock reactions for trapping of acid wastes. Appl. Geochem. 15, 1085–1095.

Gunter, W.D., Wiwchar, B., Perkins, E.H., 1997. Aquifer disposal of CO_2-rich greenhouse gases: Extension of the time scale of experiment for CO_2-sequestering reactions by geochemical modelling. Mineral. Petrol. 59, 121–140.

Harrison, W.J., Wendlandt, R.F., Sloan, E.D., 1995. Geochemical interactions resulting from carbon dioxide disposal on the sea floor. Appl. Geochem. 10, 461–475.

Hitchon, B., Gunter, W.D., Gentzis, T., Bailey, R.T., 1999. Sedimentary basins and greenhouse gases: a serendipitous association. Energy Convers. Mgmt. 40, 825–843.

Holloway, S., 1997a. An overview of the underground disposal of carbon dioxide. Energy Convers. Mgmt. 38 (SS), S193–S198.

Holloway, S., 1997b. Safety of the underground disposal of carbon dioxide. Energy Convers. Mgmt 38 (SS), S241–S245.

Holloway, S., Rochelle, C.A., Pearce, J.M., 1999. Geological sequestration of carbon dioxide: implications for the coal industry. Trans. Inst. Mining Metal. Sec. B-Appl. Earth Sci. 108, B19–B22.

Hurter, S.J., Pollack, H.N., 1996. Terrestrial heat flow in the Parana Basin, southern Brazil. J. Geophys. Res. 101, 8659–8671.

Janecky, D.R., 1982. Serpentinization of Peridotite within the Oceanic Crust: Experimental and Theoretical Investigations

of Seawater-peridotite Interaction at 200 °C and 300 °C, 500 Bars. PhD Thesis, Univ. Minnesota.

Johansson, T.B., Williams, R.H., Ishitani, H., Edmonds, J.A., 1996. Options for reducing CO_2 emissions from the energy supply sector. Energy Policy 24, 985–1003.

Kaszuba, J.P., Janecky, D.R., 2000. Experimental hydration and carbonation reactions of MgO: a simple analog for subsurface carbon sequestration processes. Geol. Soc. Am., Abstr. with Prog. 32, A202.

Kaszuba, J.P., Janecky, D.R., Snow, M.G., 2001. Carbon dioxide reaction processes in a model brine aquifer at 200 C and 200 bars: implications for subsurface carbon sequestration. Geol. Soc. Am., Abstr. with Prog. 33, A232.

Koide, H., Shindo, Y., Tazaki, Y., Iijima, M., Ito, K., Kimura, N., Omata, K., 1997. Deep sub-seabed disposal of CO_2: the most protective storage. Energy Convers. Mgmt. 38 (SS), S253–S258.

Lake, L.W., 1989. Enhanced Oil Recovery. Prentice Hall. Englewood Cliffs, NJ.

Lindeberg, E., 1997. Escape of CO_2 from aquifers. Energy Convers. Mgmt. 38 (SS), S235–S240.

Lucien, F.P., Foster, N.R., 2000. Solubilities of solid mixtures in supercritical carbon dioxide: a review. J. Supercrit. Fluids 17, 111–134.

Malinin, S.D., 1959. The system water-carbon dioxide at high temperatures and pressures. Geochem. Internat. 3, 292–306.

McBride, E.F., Milliken, K.L., Cavazza, W., Cibin, U., Fontana, D., Picard, M.D., Zuffa, G.G., 1995. Heterogeneous distribution of calcite cement at the outcrop scale in Tertiary Sandstones, Northern Apennines, Italy. AAPG Bull. 79, 1044–1063.

McPherson, B.J.O.L., Cole, B.S., 2000. Multiphase CO_2 flow, transport and sequestration in the Powder River Basin, Wyoming, USA. J. Geochem. Explor. 69-70, 65–69.

Milliken, K.L., 2001. Diagenetic heterogeneity in sandstone at the outcrop scale, Breathitt Formation (Pennsylvanian), eastern Kentucky. AAPG Bull. 85, 795–815.

Oldenburg, C.M., Pruess, K., Benson, S.M., 2001. Process modeling of CO_2 injection into natural gas reservoirs for carbon sequestration and enhanced gas recovery. Energy Fuels 15, 293–298.

Perkins, E.H., Gunter, W.D., 1995. Aquifer disposal of CO_2-rich greenhouse gasses: modelling of water-rock reaction paths in a siliciclastic aquifer. In: Kharaka, Y.K., Chudaev, O.V. (Eds.), Proc. 8th Internat. Symp. Water-Rock Interaction. A.A. Balkema, pp. 895–898.

Raymond, L.A., 2002. Petrology: The Study of Igneous, Sedimentary and Metamorphic Rocks. McGraw-Hill, New York.

Schultz, J.L., Boles, J.R., Tilton, G.R., 1989. Tracking calcium in the San Joaquin basin, California: a strontium isotopic study of carbonate cements at North Coles Levee. Geochim. Cosmochim. Acta 53, 1991–1999.

Seyfried W.E., Jr., 1977. Seawater-basalt Interaction from 25°-300 °C and 1-500 Bars: Implications for the Origin of Submarine Metal-bearing Hydrothermal Solutions and Regulation of Ocean Chemistry. PhD Thesis, Univ. Southern California.

Seyfried, W.E., Jr., Janecky, D.R., Berndt, M.E., 1987. Rocking autoclaves for hydrothermal experiments, II. The flexible reaction-cell system. In: Ulmer, G.C., Barnes, H.L. (Eds.), Hydrothermal Experimental Techniques. John Wiley & Sons, pp. 216–239.

Shyu, G.S., Hanif, N.S.M., Hall, K.R., Eubank, P.T., 1997. Carbon dioxide-water phase equilibria results from the Wong-Sandler combining rules. Fluid Phase Equilib. 130, 73–85.

Span, R., Wagner, W., 1996. A new equation of state for carbon dioxide covering the fluid region from the triple-point temperature to 1100 K at pressures up to 800 MPa. J. Phys. Chem. Ref. Data 25, 1509–1596.

Stein, C.L., Krumhansl, J.L., 1988. A model for the evolution of brines in salt from the lower Salado Formation, southeastern New Mexico. Geochim. Cosmochim. Acta 52, 1037–1046.

Takenouchi, S., Kennedy, G.C., 1964. The binary system H_2O-CO_2 at high temperatures and pressures. Am. J. Sci. 262, 1055–1074.

Todheide, K., Franck, E.U., 1963. Das Zweiphasengebiet und die kritische kurve in system kohlendioxide-wasser bis zu drucken von 3500 bar. Z. Phys. Chem. (Neue Folge) 37, 387–401.

Ward's Natural Science Establishment I., 1970. Manual for Ward's Collection of Classic North American Rocks, 45 W 7217. Rochester, NY.

Wilson, A.M., Boles, J.R., Garven, G., 2000. Calcium mass transport and sandstone diagenesis during compaction-driven flow: Stevens Sandstone, San Joaquin basin, California. Geol. Soc. Am. Bull. 112, 845–856.

Wolery T.J., 1992. EQ3NR, A Computer Program for Geochemical Aqueous Speciation-solubility Calculations: Theoretical Manual, User's Guide, and Related Documentation (Version 7.0), UCRL-MA-110662 PT III. Livermore, CA.

Wood, J.R., Boles, J.R., 1991. Evidence for episodic cementation and diagenetic recording of seismic pumping events, North Coles Levee, California, USA. Appl. Geochem. 6, 509–521.